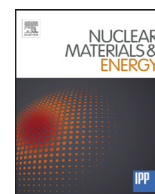


Contents lists available at [ScienceDirect](http://ScienceDirect)

# Nuclear Materials and Energy

journal homepage: [www.elsevier.com/locate/nme](http://www.elsevier.com/locate/nme)

## Influence of an external magnetic field on damage by self-ion irradiation in Fe<sub>90</sub>Cr<sub>10</sub> alloy

Fernando José Sánchez<sup>a,\*</sup>, Isabel García-Cortés<sup>a</sup>, José Francisco Marco<sup>b</sup>,  
David Jiménez-Rey<sup>a,c</sup>, Aránzazu Maira<sup>c</sup>, Jesús Castellanos<sup>a</sup>, Rafael Vila<sup>a</sup>, Ángel Ibarra<sup>a</sup>

<sup>a</sup>Laboratorio Nacional de Fusión, CIEMAT, Avda. Complutense 40, 28040 Madrid Spain

<sup>b</sup>Instituto de Química Física "Rocasolano", CSIC, Calle Serrano 119, 28006 Madrid Spain

<sup>c</sup>Centro de Micro Análisis de Materiales-UAM, Calle Faraday 3, Cantoblanco, 28049 Madrid Spain

### ARTICLE INFO

#### Article history:

Received 11 November 2015

Revised 11 March 2016

Accepted 17 May 2016

Available online xxx

#### Keywords:

Fe–Cr alloys

Self-ion irradiation

External magnetic field

Mössbauer spectroscopy

Cr clustering

### ABSTRACT

The effect of an external magnetic field ( $B=0.5$  T) on Fe<sub>90</sub>Cr<sub>10</sub> specimens during Fe ion irradiation, has been investigated by means of Conversion Electron Mössbauer Spectroscopy (CEMS). The analysis has revealed significant differences in the average hyperfine magnetic field ( $\langle \Delta H \rangle = 0.3$  T) between non-irradiated and irradiated samples as well as between irradiations made with  $B$  (w/  $B$ ) and without  $B$  (w/o  $B$ ). It is considered that these variations can be due to changes in the local environment around the probe nuclei (<sup>57</sup>Fe); where vacancies and Cr distribution play a role. The results indicate that the Cr distribution in the neighbourhood of the iron atoms could be changed by the application of an external field. This would imply that an external magnetic field may be an important parameter to take into account in predictive models for Cr behaviour in Fe–Cr alloys, and especially in fusion conditions where intense magnetic fields are required for plasma confinement.

© 2016 The Authors. Published by Elsevier Ltd.

This is an open access article under the CC BY-NC-ND license

(<http://creativecommons.org/licenses/by-nc-nd/4.0/>).

### 1. Introduction

In magnetic confinement fusion reactor devices the vacuum vessel and structural materials will need to withstand intense and hazardous radiation environments in the presence of the strong magnetic fields (up to several Tesla) required for plasma confinement. At present, high-chromium ferritic/martensitic steels are candidate structural materials for such devices. One reason for selecting these steels as reactor materials is their superior resistance to irradiation, in terms of low damage accumulation and relatively low swelling [1,2]. In principle, the micro-structural and mechanical properties of materials are modified by the propagation of defects produced under irradiation [3]. Moreover, several theoretical works point to the local magnetism as an important parameter in the atom distribution and in the kinetics of interstitial formation in FeCr alloys [4,5,6]. All these studies point to the importance of including the presence of external magnetic fields when considering irradiation damage in such materials. To date, the effect of the magnetic field,  $B$ , has not been taken into account in experiments emulating radiation damage in candidate fusion materials.

Thus, expanded experimental knowledge of structural material response to irradiation under magnetic fields has become critical.

This work discusses the first experimental results obtained for a series of Fe<sub>90</sub>Cr<sub>10</sub> alloy specimens irradiated with 1 MeV Fe<sup>+</sup> ions under the effect of the magnetic field produced by a permanent magnet (0.5 T) and analysed by Mössbauer Spectroscopy.

### 2. Experimental

A set of experiments to investigate the influence of an external magnetic field on ion induced damage have been carried out at Centro de MicroAnálisis de Materiales (CMAM) [7] irradiation facility. In the experiments Fe<sub>90</sub>Cr<sub>10</sub> alloy samples have been irradiated in pairs with and without external magnetic field ( $B=0.5$  T) using a dedicated custom sample holder with a permanent magnet embedded behind one of the samples (Fig. 1). The magnetic field lines are oriented normal to the sample surface in order to avoid ion beam spreading. Commissioning of the system was performed at CMAM by the irradiation of a luminescent material deposited on a metal support plate. In this way, it was observed that the ions impacting on the luminescent material showed good magnetic field uniformity. In addition, the complete system, i.e. the holder, the permanent magnet and a UHP-Fe test sample were also tested

\* Corresponding author.

E-mail address: [fernandojose.sanchez@ciemat.es](mailto:fernandojose.sanchez@ciemat.es) (F.J. Sánchez).

<http://dx.doi.org/10.1016/j.nme.2016.05.010>

2352-1791/© 2016 The Authors. Published by Elsevier Ltd. This is an open access article under the CC BY-NC-ND license (<http://creativecommons.org/licenses/by-nc-nd/4.0/>).

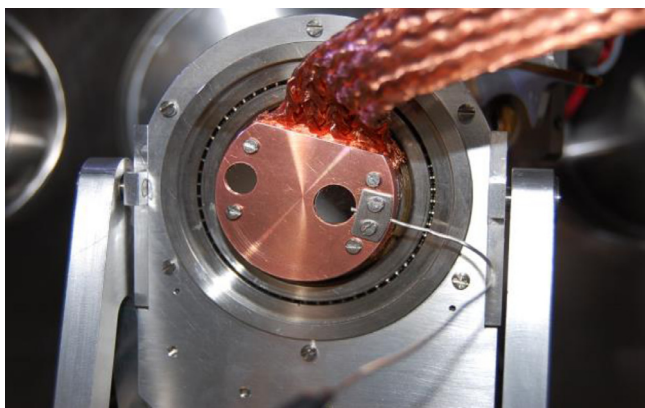


**Fig. 1.** Experimental two-sample holder. It has a permanent magnet behind the right FeCr sample. The set-up is connected to a LN cooled finger to achieve low temperature if required.

during 4 h of irradiation by a 2 MeV, 231 nA current  $H^+$  beam at a sample temperature of  $-100^\circ\text{C}$ , with and without magnetic field, getting a good temperature control during irradiation and a same ion beam footprint in sample w/o  $B$  and w/  $B$ . Although irradiations can generally be performed at low temperature, the analysis is always carried out at room temperature (RT).

In parallel, prior to starting the experiments, ANSYS simulations were done for  $\text{Fe}_{90}\text{Cr}_{10}$  slice (1 mm thick) embedded in the centre of a long solenoid (giving 1 T in the central column) in order to emulate the effect of  $B$  on the surface of the sample. Fig. 2 shows that although a high concentration of magnetic field lines are observed at the edge, there is good magnetic flux uniformity about the irradiated zone (sample central region), thus validating the experimental set-up for use with these samples.

Samples investigated here were prepared from EFDA/EURATOM type FeCr alloys ( $\text{Fe}_{90}\text{Cr}_{10}$ ). They were delivered in the form of 10.9 mm diameter bars, in a re-crystallized state after cold reduction of 70% and then heat treated for 1 h under pure argon flow at temperatures of  $850^\circ\text{C}$  followed by air cooling. For these experiments, 1 mm thick slices were cut from each bar by spark erosion and thinned by grinding and polishing in a plane-parallel polishing machine to a final thickness of  $300\mu\text{m}$  each. These specimens were irradiated at  $-100^\circ\text{C}$  in couples using 1 MeV  $\text{Fe}^+$ . The integral value of the dose reached for each sample was 15 dpa. Details of damage profiles calculated using SRIM code [8] are shown in Fig. 3.

As the ion penetration depth in these experiments is in the range of 350 nm, Mössbauer spectra have been measured by recording conversion electrons in backscattering geometry using a

conventional constant acceleration spectrometer, a  $^{57}\text{Co}(\text{Rh})$  source and a parallel plate avalanche counter [9]. For this the incident  $\gamma$ -rays were oriented to be perpendicular to the foil plane. The velocity scale was calibrated using a 6 mm  $\alpha$ -Fe foil and the isomer shifts were referenced to the centroid of the spectrum of  $\alpha$ -Fe at room temperature.

### 3. Results and discussion

#### 3.1. Spectrum analysis (CEMS)

Spectra of all specimens (as received (A.R.), irradiated without  $B$  (w/o  $B$ ) and irradiated with  $B$  (w/  $B$ )) have been analysed following the same procedure used in previous studies [10–13], i.e. with the two-shell model [14] where it was assumed that only Cr atoms situated within the 1NN and 2NN neighbour-shells cause measurable changes in spectral parameters i.e. the hyperfine field,  $H$ , and the isomer shift,  $IS$ . It is also assumed that changes both in  $H$  and  $IS$  are additive i.e.  $X(m, n; x) = X(0, 0; x) - m\Delta X_1 - n\Delta X_2$ , where  $X = H$  or  $IS$ ,  $\Delta X_1$  and  $\Delta X_2$  stand for the change in  $X$  due to the presence of one Cr atom in 1NN and one Cr atom in 2NN, respectively, around an iron atom and  $x$  refers to the Cr concentration. For a binary alloy with a random distribution of atoms, the probability of finding  $m$  Cr atoms in 1NN and  $n$  ones in 2NN,  $P(m, n)$ , follows a binomial distribution. Within the 1NN–2NN approximation, there are  $N=63$  ( $m, n$ ) possible configurations for the BCC structure, with 8 first neighbours and 6 second neighbours (Fig. 4). In this case, in order to fulfil the condition:  $(m, n; x) > 0.97$ , the number  $N$  of possible configurations is significantly reduced to 11 ( $x = 10$ ) [14]. Therefore, the spectra of the samples were fitted to a superposition of 11 sextets with different hyperfine parameters, depending on the number of neighbours for the iron atoms. As described above, taking into account the mentioned additive rule, we started with values  $H(0,0) = 33.7$  T,  $IS(0,0) = 0.00$   $\text{mms}^{-1}$ ,  $\Delta H_1 = -3.1$  T,  $\Delta H_2 = -2.0$  T,  $\Delta IS_1 = -0.022$   $\text{mms}^{-1}$  and  $\Delta IS_2 = -0.009$   $\text{mms}^{-1}$  [11]. In order to avoid divergences in the fit all the spectra were fitted having the same linewidth.

Examples of spectra are shown in Fig. 5. Besides the 11 sextets, a paramagnetic doublet was also included in the fit of all the spectra. The Mössbauer parameters of these doublets ( $QS = 0.31$ – $0.40$   $\text{mms}^{-1}$ ;  $IS = 0.75$ – $0.95$   $\text{mms}^{-1}$ ), whose relative areas amount to 5–7% of the total spectral area, can be associated to the presence of superparamagnetic or amorphous  $\text{Fe}^{3+}$  oxyhydroxides [15]. These compounds arise habitually from a thin oxidation layer formed after the exposure of the alloys to the laboratory atmosphere [16]. Other interpretations as being due to iron dissolved in paramagnetic phases are doubtful as the corresponding isomer shifts are very large and characteristic of  $\text{Fe}^{3+}$  in octahedral oxygen coordination.

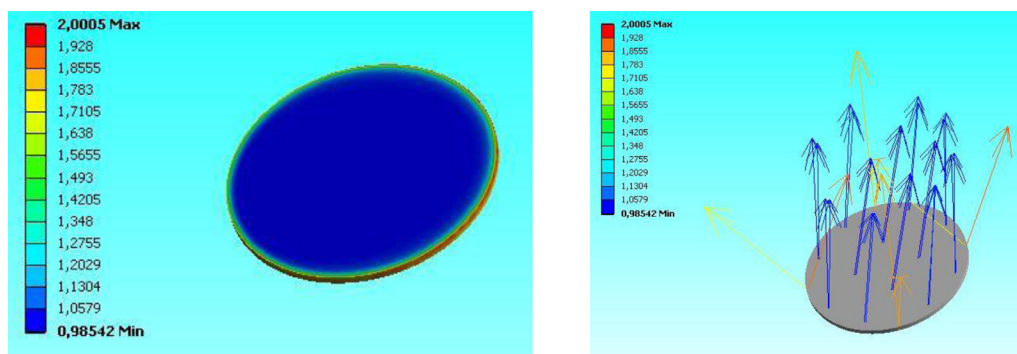


**Fig. 2.** ANSYS simulations (see text for explanation).

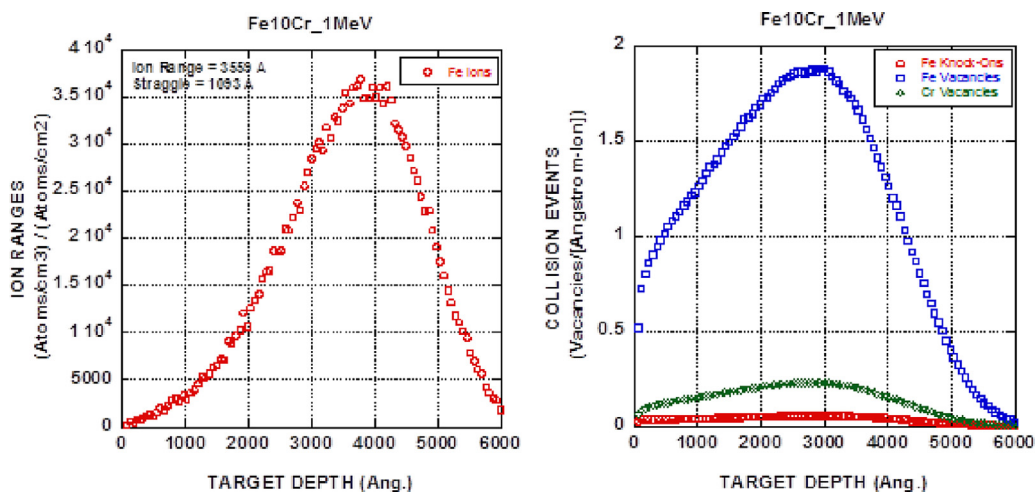


Fig. 3. SRIM 2003 calculations of ion range and damage profiles produced by 1MeV  $\text{Fe}^{+1}$  ion irradiation in  $\text{Fe}_{90}\text{Cr}_{10}$  alloys at full damage cascade and 40 eV as displacement energy.

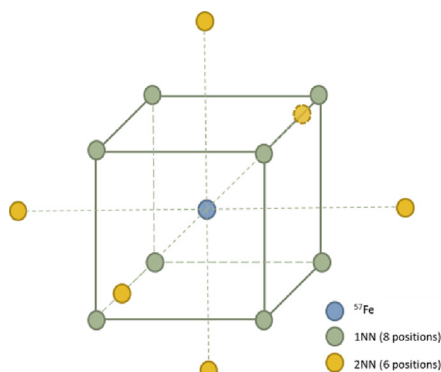


Fig. 4. BCC structure showing 1NN and 2NN atomic positions.

### 3.2. Average hyperfine magnetic field

As described above, a Mössbauer spectrum can display different components belonging to Mössbauer atoms occupying crystal sites with different neighbouring configurations. Hence, the average hyperfine field  $\langle H \rangle$  has been calculated as the weighted average of the hyperfine fields associated with particular atomic configurations, using  $\langle H \rangle = \sum_{m,n} P(m,n)H(m,n)$  where  $H(m,n)$  is the hyperfine field for a given  $(m,n)$  atomic configuration and  $P(m,n)$  is the corresponding probability of such configuration (spectral area of the respective sextet). The spectral contribution from the defects is usually overwhelmed by the contribution from Mössbauer atoms belonging to perfect crystalline regions. However it is still possible to detect significant variations in the average hyperfine field after irradiation [17]. These variations are considered to be a combined effect of vacancies generated during irradiation and the degree of Cr ordering in the alloy, i.e. if the Cr distributes in clusters due to irradiation,  $\langle H \rangle$  will increase, while short-range order (SRO) and vacancies will decrease this magnitude [10].

Fig. 6 shows the average hyperfine field of specimens before and after irradiation (both w/  $B$  and w/o  $B$ ). It is larger in both irradiated samples respect to that observed in the reference sample. This increase in the average hyperfine magnetic field is due, as the inspection of the fitted spectra reveals, to the increase in intensity of the sextets corresponding to configurations of the type (1,0) and (1,1) (third and fourth sextets) at expenses of the sextets corresponding to configurations having more Cr atoms in the

neighbourhood of the Fe atoms. The sextets corresponding to these rich Cr configurations are characterised by smaller hyperfine magnetic field values and are more important in the reference sample than in the irradiated samples (Fig. 6). Although the differences in average hyperfine field can be considered small, this difference is relevant as arises from substantially different sextet distributions from sample to sample. Therefore, the increase of  $\langle H \rangle$  for the irradiated samples (w/o and w/  $B$ ) can be explained in terms of the clustering of Cr atoms, which implies an underlying decrease of Cr concentration in the neighbourhood of the probe  $^{57}\text{Fe}$  nuclei due to  $\text{Fe}^{+}$  irradiation.

### 4. Conclusions

The irradiation of  $\text{Fe}_{90}\text{Cr}_{10}$  samples with 1 MeV  $\text{Fe}^{+}$  to a final dose of 15 dpa (integral value) has been investigated in the presence of an external magnetic field (0.5 T). As shown by Mössbauer spectroscopy, the irradiation brings about an increase of the average hyperfine field,  $\langle H \rangle$  in both irradiated samples what implies a decrease of the chromium content within the 1NN–2NN volume around the probe nuclei. The data obtained in the sample irradiated under applied magnetic field appear to show a different sextet distribution (a different population of neighbouring configurations) than in the sample irradiated without applied magnetic field what results in a slightly smaller average hyperfine magnetic field. Overall the results indicate that the irradiation caused the formation of clusters of Cr atoms in both cases.

This work presents the first results of experiments to investigate the influence of an external magnetic field in alloys that are crucial for future fusion machines. All the studied parameters indicate that the irradiation of  $\text{Fe}_{90}\text{Cr}_{10}$  samples by  $\text{Fe}^{+}$  induces clustering of Cr and that the cluster distribution can be changed by the application of an external magnetic field. Work is in progress to confirm the changes induced by external magnetic fields during irradiation considering the role of more intense fields, different irradiation conditions, as well as different Cr contents in the alloys. The results will be addressed in future articles.

### Acknowledgements

The authors would like to thank A. Muñoz for fruitful discussions and A. Rodriguez, A. Nakbi, J. Narros and V. Joco for their technical support. This work was supported by national program



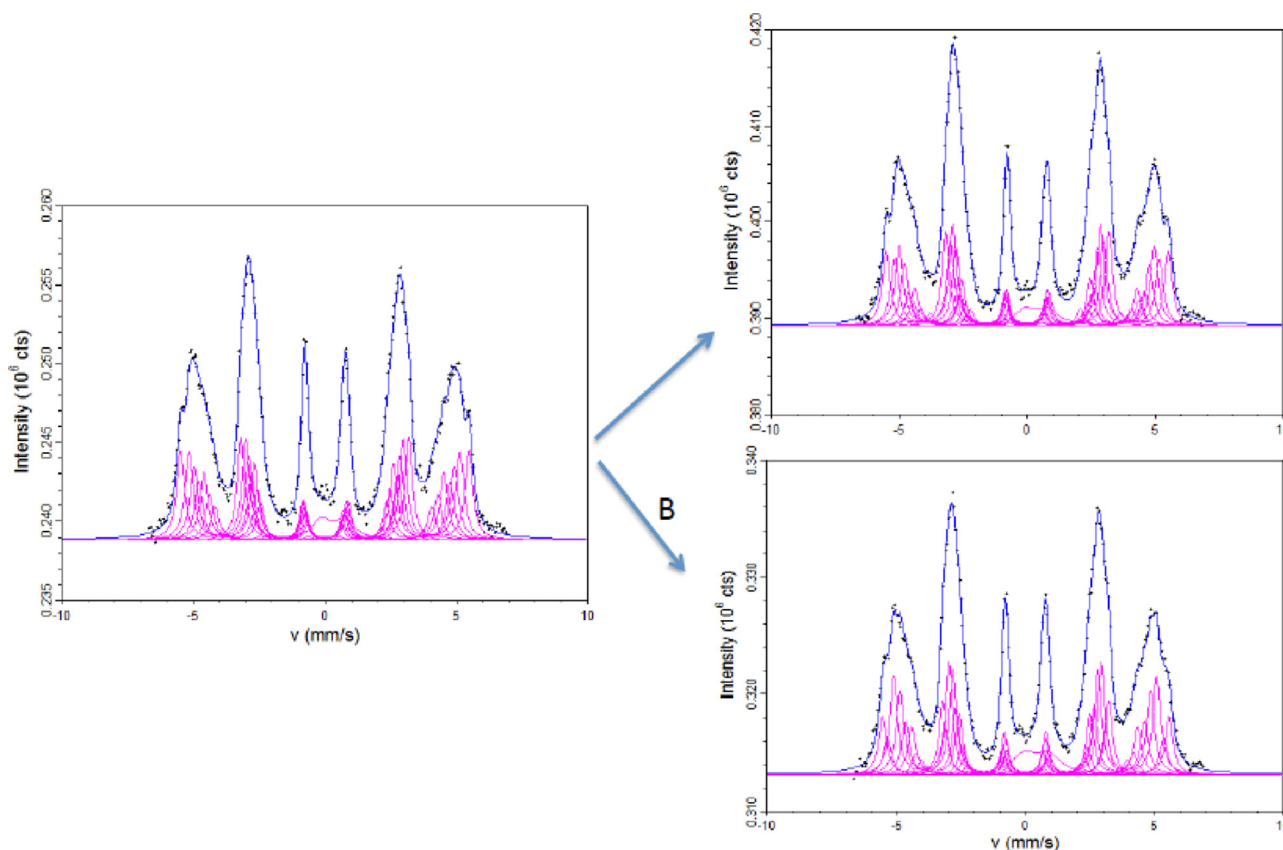


Fig. 5. Fitted Mössbauer spectra for  $\text{Fe}_{90}\text{Cr}_{10}$ : un-irradiated (left), irradiated by  $\text{Fe}^+$  w/o  $B$  (upper right) and w/  $B$  (lower right). The pink peaks are 11 sextets showing different Cr neighbouring groups (see text for explanation) “ (For interpretation of the references to colour in this figure legend, the reader is referred to the web version of this article.)”.

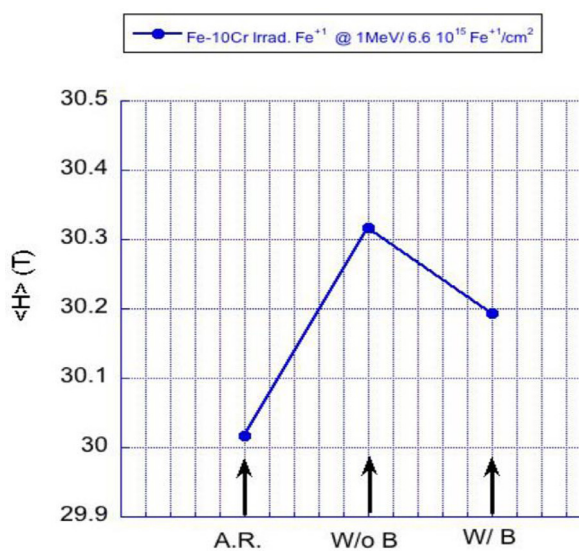


Fig. 6. Average hyperfine fields for three samples (as received, A.R., irradiated with-out and with the magnetic field).

RADIAFUS III (ENE2012-39787-C06-01) and Madrid regional government through the project TECHNOFUSION II CM (S2013/MAE-2745).

## References

- [1] E.A. Little, J. Nuc. Mat. 87 (1979) 11–24.
- [2] E.A. Little, J. Nuc. Mat. 87 (1979) 25–39.
- [3] R.L. Klueh, D.R. Harries, High-Chromium Ferritic Martensitic Steels for Nuclear Applications, ASTM, Bridgeport, 2001 ISBN 0-803102090-7.
- [4] T. Seletskaiia, Y. Osetsky, R.E. Stoller, G.M. Stocks, Phys. Rev. Lett. 94 (2005) 046403 and Phys. Rev. B 78 (2008) 134103.
- [5] A. Froideval, R. Iglesias, M. Samaras, S. Schuppler, P. Nagel, D. Grolmund, M. Victoria, W. Hoffelner, Phys. Rev. Lett. 99 (2007) 237201.
- [6] L. Malerba, J. Nuc. Mat. 382 (2008) 112–125.
- [7] A. Climent-Font, F. Pászti, G. García, M.T. Fernández-Jiménez, F. Agulló, Nucl. Instrum. Meth. B 219–220 (2004) 400–404.
- [8] J.F. Ziegler, Nucl. Instrum. Meth. B. 219–220 (2004) 1027–1036.
- [9] J.R. Gancedo, M. Gracia, J.F. Marco, Hyperfine Interactions 66 (1991) 83–93.
- [10] R. Idczak, R. Konieczny, J. Chojcan, J. Phys. and Chem. of Solids 73 (2012) 1095–1098.
- [11] S.M. Dubiel, J. Cieslak, H. Reuther, Nucl. Instrum. Meth. B 302 (2013) 48–50.
- [12] S.S. Huang, S. Kitao, Y. Kobayashi, T. Yoshiie, Q. Xu, K. Sato, M. Seto, J. Nuc. Mat. 456 (2015) 266–271.
- [13] B. Gómez-Ferrer, I. García-Cortés, J.F. Marco, D. Jiménez-Rey, R. Vila, Phys. Rev. B 90 (2014) 220102(R).
- [14] S.M. Dubiel, J. Cieslak, Phys. Rev. B 83 (2011) 180202(R).
- [15] cap. 12 E. Murad, J.H. Johnston, Iron oxides and oxyhydroxides, in: G.J. Long (Ed.), Mössbauer Spectroscopy Applied to Inorganic Chemistry, 2, Plenum Press, New York, 1987, pp. 507–582.
- [16] M. Gracia, J.F. Marco, J.R. Gancedo, W. Exel, W. Meisel, Surface Interface Anal. 29 (2000) 82–91.
- [17] S.M. Dubiel, J. Żukrowski, J. Alloys Compounds 624 (2015) 165–169.